MRS Communications (2023) 13:1187–1195
© The Author(s), under exclusive licence to The Materials Research Society, 2023
https://doi.org/10.1557/s43579-023-00427-1

MRS Communications

Research Letter

Element doping improving mechanical properties of β' phase in Al–Mg–Si alloy

Jin Wang, National Center for Materials Service Safety, University of Science and Technology Beijing, Beijing 102206, China
Lianhong Ding, School of Information, Beijing Wuzi University, Beijing 101149, China
Mengmeng Duan, and Chuan-Hui Zhang, National Center for Materials Service Safety, University of Science and Technology Beijing, Beijing 102206, China

Address all correspondence to Lianhong Ding at **lhdingbwu@sina.com** and Chuan-Hui Zhang at **zhangch@ustb.edu.cn**

(Received 5 April 2023; accepted 1 August 2023; published online: 22 August 2023)

Abstract

The effect of element doping on the mechanical properties of β′-Mg_9Si_5 phase in Al–Mg-Si alloys are investigated using density-functional calculations. The results reveal that $Mg_{17}Si_{10}Ge$ exhibits the highest degree of stability, attributed to its lower formation enthalpies. Doping of Ge and Zn elements may lead to a reduction in the material's hardness. Conversely, the addition of Al and Zn elements can significantly enhance the toughness and ductility of $Mg_{17}Si_{10}X$. The electron orbits of Si atoms are the primary influencing factor. The strength-ductility of these materials can be finely tuned by altering the charge transfer around the doping atoms.

Introduction

Al–Mg–Si alloys are widely used in structural applications due to their high strength-to-weight ratio and excellent corrosion resistance. During a specific heating treatment process, the existence of various nano-sized needle- or plate-like metastable precipitates in the aluminum matrix significantly impedes the motion of dislocations, thereby improving the mechanical property of alloys.[1]

The rod-like β' phase is known to appear in over-aged specimens of Al–Mg–Si alloys and has a hexagonal structure with a composition of Mg_9Si_5.[2] In recent years, researchers have become increasingly interested in the β' phase.[3] as it is believed to play a crucial role in hardening commercial Al alloys by forming fine, coherent precipitates within the Al matrix without boundaries. The β' phase coexists at least two other phases, U1 and U2, and has a structure with more Si atoms along the hexagonal *c* axis (4/3 times more), resulting in a very favorable formation enthalpy. Structural refinements reveal a significant variance in Mg-Si and Si–Si bond lengths, which introduces bond disorder. Additionally, unlike the stoichiometric Mg_2Si, the charge balance in Mg_9Si_5 is maintained through a strongly knit covalent Si network. As previously mentioned, these structural characteristics are highly desirable in structural mechanics and thermoelectric material design.[4]

Adding other microalloying elements is a common method to improve the properties of Al–Mg–Si alloys and broaden their industrial application by to change the original precipitate phase types, number density, morphology and size.[1] Some addition elements have been shown to exist in integrated Al–Mg–Si alloys, and some have been found inside and at the boundary of the precipitated phase. Through SEM tests, Zheng et al.[5] observed that the addition of Ca would precipitated Al_2Ca phase in Al–Mg–Si alloys, and a small amount of Ca would also be evenly distributed in the microstructure of the alloy. Sr used as a refiner in Al–Mg–Si alloys was reported by Lu et al.[6] They found that Sr elements uniformly distributed in the alloy would refine grains, promote precipitation and increase the forming properties of alloys. Based on the diffusion kinetics of various solute-vacancy complexes, Liu et al.[7] found that Ge notably retards the ageing kinetics of Al–Mg–Si alloys by Positron Annihilation Lifetime Spectroscopy (PALS), but the location of Ge was not characterized. A few years later, Bjørge eta al. proved the formation of Ge containing hardening phases which are isostructural with the β' and U1 phases in the Al–Mg–Si alloys.[8] It is well known that Cu, Zn, and Al have been directly observed in almost every phase of aging and in every component of Al–Mg–Si alloys.[1,9] In particular, the composition and structure of the β' phase changes because the Zn atom enter into the phase was reported.[1] In the aging process, β' is precipitated after β'', so the eutectic structure will affect the plastic deformation mechanism of precipitation-strengthened Al–Mg–Si alloy.[10] Therefore, the better mechanical properties are due to a refiner precipitation of β', and proposed that addition elements, such as Cu and Zn, are incorporated in this precipitates.[11] The above work directly or indirectly confirmed the possibility of the existence of trace elements of Ca, Sr, Al, Ge, Cu, and Zn in β' phase of Al–Mg–Si alloys. At the same time, the β' phase containing doping elements can influence the mechanical properties of the alloy.

First-principles calculations represent a valuable approach to predicting the structural and thermodynamic properties of metallic materials.[12] Through first-principles calculations, numerous studies have been published on the energetic and thermodynamic properties of stable and metastable phases

within the Al–Mg–Si system.[13,14] Researchers have previously focused on studying the structural and thermodynamic stability of the β' phase precipitates in Al–Mg–Si alloys. However, more recent research has explored other properties, such as the impact of trace element doping on the properties of the β' phase.[15] This study aims to investigate the effects of doping elements, including Ca, Sr, Al, Ge, Cu, and Zn, on the structural stability and mechanical properties of the β' phase Mg_9Si_5 phase using density-functional theory calculations. By doing so, the researchers aim to provide insights that could potentially aid in the development and performance improvement of Al–Mg–Si alloys.

Calculation methods

The electronic structure calculations of β'-Mg_9Si_5 and doped $Mg_{17}Si_{10}X$ (where X = Ca, Sr, Al, Ge, Cu, Zn) were calculated using density-functional theory (DFT) with the Cambridge Sequential Total Energy Package (CASTEP) and the ultra-soft pseudopotential method.[16] The Perdew-Burke-Ernzerh functional (PBE) was employed to treat the electron exchange and correlation potential with the generalized gradient approximation (GGA).[17] To ensure accurate results, a series of convergence tests were carried out, including varying the kinetic-energy cutoff and k-point sampling. The optimal parameters for both the pristine Mg_9Si_5 and doped $Mg_{17}Si_{10}X$ structures were found to be a cutoff energy of 500 eV and a $3 \times 3 \times 2$ k-point mesh.[18] To meet the convergence criteria, the Broyden, Fletcher, Goldfarb, and Shannon (BFGS) method.[19] was used with the following thresholds: the energy change converged to less than 1.0×10^{-5} eV/atom, the force less than 0.03 eV/Å, and the maximum displacements within 0.001 Å. Additionally, the Bader analysis was employed to calculate the charge transfer.[20]

Results and discussion

Geometric structure and energy stability

Figure S1a-S1b depict the optimized crystal structure of Mg_9Si_5 containing 18 atoms in the primitive cell. To comprehensively examine the effect of doping on Mg_9Si_5 crystal, different doped models are considered, as shown in Fig. S1c. The pristine Mg_9Si_5 crystal has five doping sites, namely Mg1, Mg2, Si1, Si2a, and Si2b. Firstly, we investigated the corresponding lattice parameter after geometry optimization for pristine Mg_9Si_5, which was found to be in agreement with the experimental[4] and other theoretical.[3,13,14] values. These results demonstrate the reliability of our parameter settings and provide a theoretical basis for subsequent doping calculation. It should be noted that doping with different elements results in different $Mg_{17}Si_{10}X$ (X = Ca, Sr, Al, Ge, Cu, Zn) models. To determine the substitution preference in the doped $Mg_{17}Si_{10}X$ compounds, we calculated and compared the formation enthalpy (ΔH_f) and cohesive energy (E_{coh}) upon with different elements.

In our calculations, the enthalpy of formation (ΔH_f) and cohesive energy (E_{coh}) are defined as follows:

$$\Delta H_f = \frac{E_{tot} - N_{Mg}E_{Mg} - N_{Si}E_{Si} - N_X E_X}{N_{Mg} + N_{Si} + N_X} \quad (1)$$

$$E_{coh} = \frac{E_{tot} - N_{Mg}E_{atom}^{Mg} - N_{Si}E_{atom}^{Si} - N_X E_{atom}^{X}}{N_{Mg} + N_{Si} + N_X}, \quad (2)$$

where E_{tot} are the total energies of doped $Mg_{17}Si_{10}X$ and $Mg_{18}Si_9X$ compounds, E_{Mg}, E_{Si} and E_x are the energies of respective atoms in bulk, and the $E^{Mg}{}_{atom}$, $E^{Si}{}_{atom}$, $E^{x}{}_{atom}$ are the energies of isolated atoms. N_{Mg}, N_{si}, N_x denote the number atoms. Our calculated results indicate that the doping elements Ca, Sr, Al, Ge, Cu, and Zn preferentially occupy the Mg2 site due to their lowest formation enthalpy and cohesive energy values. This finding is supported by the data presented in Table SI and Fig. 1. Furthermore, our calculations for the formation enthalpy and cohesive energy of β'-Mg_9Si_5 are consistent with theoretical values cited in the literature.[3,13,14,21] We also

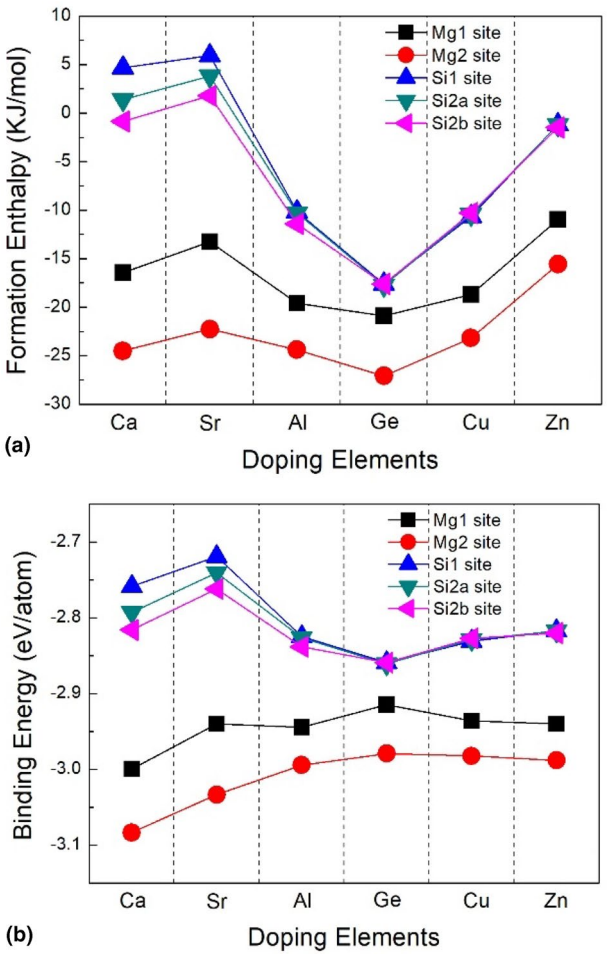

Figure 1. Formation enthalpy and Binding energy of doped $Mg_{17}Si_{10}X$ structures (X=Ca, Sr, Al, Ge, Cu, Zn).

observed that the values of ΔH_f for $Mg_{17}Si_{10}X$ follow the trend: $Mg_{17}Si_{10}Zn$ (− 15.578 kJ/mol) < $Mg_{17}Si_{10}Sr$ (− 22.250 kJ/mol) < $Mg_{17}Si_{10}Cu$ (− 23.171 kJ/mol) < $Mg_{17}Si_{10}Al$ (− 24.384 kJ/mol) < $Mg_{17}Si_{10}Ge$ (− 27.085 kJ/mol). Notably, $Mg_{17}Si_{10}Ge$ has the lowest formation enthalpy, indicating that this configuration is the most stable. Overall, these results suggest that doping atoms can exist stably in the β'-Mg_9Si_5 phase.

Effect of doping on mechanical properties

The mechanical properties of materials, including their brittleness, ductility, and hardness, can be evaluated by the mechanical parameters calculated through elastic constant, such as bulk modulus, Young's modulus and shear modulus.[22] The following parts mainly focus on the elastic properties of $Mg_{17}Si_{10}X$ (X = Ca, Sr, Al, Ge, Cu, Zn) compounds. For C14-type β'-Mg_9Si_5 phase, six independent elastic constants (C_{11}, C_{12}, C_{13}, C_{33}, C_{44}, C_{66}) were calculated to evaluate the resistance of a crystal to externally applied stress. The mechanical stability condition are as follows due to it belongs to hexagonal structures [22]:

$$C_{11} > 0,\ C_{11} - C_{12} > 0,\ C_{44} > 0,\ (C_{11} - C_{12})C_{33} - 2C_{13}^2 > 0 \quad (3)$$

Table SII shows the elastic constants of pristine Mg_9Si_5 and $Mg_{17}Si_{10}X$ compounds, where X represents various doping elements including Ca, Sr, Al, Ge, Cu, and Zn. Our calculated elastic constants for pristine Mg_9Si_5 are consistent with the first-principles data calculated by Zhang B. et al.[23] This suggests that the calculated results of elastic constant for the $Mg_{17}Si_{10}X$ compounds should also be adopted on the basic of the results of the pristine phase. From Table SII, it is observed that the elastic constants of all structures satisfy the thermodynamic stability criterion in Eq. (3). This implies that all the $Mg_{17}Si_{10}X$ compounds are mechanically stable at low temperature, which is consistent with the previously calculated results of the formation enthalpy.

Moreover, doping of elements in the $Mg_{17}Si_{10}X$ compounds can significantly impact the mechanical properties such as bulk modulus (B), shear modulus (G), Young's modulus (E) and Poisson ratio (ν). These properties can be evaluated using the following equation.[24]

$$E = 9BG/(3B + G) \quad (4)$$

$$\nu = (3B - 2G)/(6B + 2G) \quad (5)$$

A series of data are listed in Table I based on Eqs. (4) and (5). It is worth noting that our calculations of B and G for Mg_9Si_5 are close to the experimental data obtained through the fitting of equation of state at 0 K (without zero-point vibrational energy).[25] With the addition of doping atoms (Ca, Al, Ge and Cu), the bulk modulus of Mg_9Si_5 has not changed significantly. However, the doping of Zn leads to a smaller bulk modulus for Mg_9Si_5, indicating a relatively weaker ability to resist volume deformation and improve the strength of Mg_9Si_5. Overall, it is apparent that the doping elements greatly decrease shear modulus of the Mg_9Si_5 phase. Specifically, the doping of Zn decreases the shear modulus by 30%, implying that the toughness of $Mg_{17}Si_{10}Zn$ compound is reduced.

The B/G ratio, which represents the ratio of bulk modulus to shear modulus, is a fundamental quantity used to predict whether a material will exhibit brittle or ductile behavior. Pugh.[25] proposed a critical value of 1.75 to estimate this ratio. The doping of Ge, Cu, and Zn elements in the Mg_9Si_5 phase increases the B/G values, implying a slight increase in brittleness. However, the shear modulus of the Mg_9Si_5 phase decreases due to the doping of Ge, Cu and Zn elements, which means that it may not become a harder material. In contrast, there are minimal changes to the B/G ratio of the Mg_9Si_5 phase before or after doping with Ca and Sr elements, indicating that the doping of those elements could improve the ductility of the Mg_9Si_5 phase while losing less strength. Furthermore, the doping of Al elements results in the B/G value of Mg_9Si_5 phase reaching the critical value of 1.75, indicating that it could improve the ductility of the Mg_9Si_5 phase without affecting its strength.

We also calculated Young's modulus and Poisson ratio of the doped Mg17Si10X compounds, which are used to measure the ability of the material to resist uniaxial compression and

Table I. Mechanical parameters of pristine Mg_9Si_5 and $Mg_{17}Si_{10}X$ structures (X = Ca, Sr, Al, Ge, Cu, Zn).

Structures	B_V (GPa)	B_R (GPa)	B (GPa)	G_V (GPa)	G_R (GPa)	G (GPa)	E (GPa)	B/G	ν	A_u	H_V (GPa)
Mg_9Si_5	56.9	56.9	56.9	40.7	38.3	39.5	96.2	1.44	0.211	0.317	8.67
Cal. [3]	56.9	56.8	56.9	39.9	34.9	37.4	92.0	1.52	0.23	0.71	
Cal. [2]			58.0								
Cal. [13]			59.95								
$Mg_{17}Si_{10}Ca$	56.0	56.0	56.0	39.1	37.1	38.1	93.1	1.47	0.217	0.271	8.18
$Mg_{17}Si_{10}Sr$	54.8	54.7	54.8	37.8	35.9	36.9	90.2	1.49	0.220	0.268	7.89
$Mg_{17}Si_{10}Al$	57.0	57.0	57.0	33.4	31.7	32.6	82.0	1.75	0.255	0.280	6.01
$Mg_{17}Si_{10}Ge$	56.9	56.8	56.9	36.2	33.4	34.8	86.7	1.63	0.237	0.435	6.99
$Mg_{17}Si_{10}Cu$	57.0	56.8	56.9	37.8	35.2	36.5	90.2	1.56	0.228	0.370	7.55
$Mg_{17}Si_{10}Zn$	48.4	41.7	45.1	32.0	23.4	27.7	68.9	1.63	0.229	1.998	6.69

plasticity, respectively. In Table I, our results show that the Young's modulus of the doped $Mg_{17}Si_{10}X$ compounds is lower than that of the pristine phase (96.2 GPa), while the Poisson's ratios of the doped $Mg_{17}Si_{10}X$ compounds are all higher than that of the pristine phase (0.211). These findings indicate that the doping of elements sacrifices the strength of the pristine phase for better plasticity, especially for the doping of Al, Ge, Zn, which exhibit a lower Young's modulus and higher Poisson's ratio.

Furthermore, the Vickers hardness (H_V) of the material was considered using the following formula.[26]

$$H_V = 0.92(G/B)^{1.137}\, G^{0.708} \quad (6)$$

Table I shows that the H_V values of the $Mg_{17}Si_{10}X$ compounds range from 6.01 to 8.18 GPa, which are lower compared to the pristine Mg_9Si_5 phase. This indicates that doping with Ca, Sr, Al, Ge, Cu and Zn elements reduces the hardness of the Mg_9Si_5 phase. Among them, the hardness of $Mg_{17}Si_{10}Ca$ and $Mg_{17}Si_{10}Sr$ compounds decreased slightly, while the three structures of $Mg_{17}Si_{10}Al$, $Mg_{17}Si_{10}Ge$ and $Mg_{17}Si_{10}Zn$ decreased the most. Our calculated results confirm the conclusions about the impact of doping on the ductility and plasticity for the Mg_9Si_5 phase.

In this paragraph, the universal elastic anisotropy index (A^U) is calculated and discussed. This index is an important factor in the formation of microcracks and lattice distortion in materials, and is used to study their mechanical properties.[27] The equation for calculating the A^U value is given.

$$A^U = 5G_V/G_R + B_V/B_R - 6 \quad (7)$$

After obtaining a higher G_R value, it is evident that the calculated A^U value of the pristine Mg_9Si_5 phase is 0.317, which is lower than that of 0.71 reported by Zhang B. et al. [23]. Table I reveals that the A^U values of all structures are not equal to zero, indicating that the Mg_9Si_5 phase is anisotropic. Furthermore, the anisotropic properties of doped $Mg_{17}Si_{10}X$ compounds with Ge and Zn are more pronounced than those of the pristine phase. Notably, for $Mg_{17}Si_{10}Zn$ phase exhibits significantly stronger anisotropic properties than the pristine phase due to its larger A^U value. This finding suggests that $Mg_{17}Si_{10}Zn$ compound has the strongest resistance to crack initiation. In comparison with other doped elements, the A^U values of the Mg_9Si_5 phase after Ca, Sr and Al elements doping are closer to zero, implying that they have weaker abilities to resist crack initiation.

The Debye temperature (Θ_D),[28] which can be used to qualitatively judge the stability of lattice vibration, hardness, and bonding strength of materials, is estimated using the following equations.[29]

$$\Theta_D = \frac{h}{k_B}\left[\frac{3n}{4\pi}\left(\frac{N_A\rho}{M}\right)\right]^{1/3} v_m \quad (8)$$

$$v_m = \left[\frac{1}{3}\left(\frac{2}{v_s^3} + \frac{1}{v_l^3}\right)\right]^{-1/3},\ v_l = \sqrt{\left(B + \frac{4}{3}G\right)\frac{1}{\rho}},\ v_s = \sqrt{G/\rho}, \quad (9)$$

where h and k_B are the Planck and Boltzmann constants, respectively. n is the total number of atoms per formula, N_A and M are the Avogadro number and the molecular weight per formula, respectively, and v_m, v_l, and v_s are the average sound velocity, longitudinal sound velocity and shear sound velocity, respectively.

Table SIII shows that the Θ_D of the Mg_9Si_5 phase is 518.54, which is consist with other results. [14,30] The Θ_D of the Mg_9Si_5 phase decreases after doping with other elements, indicating that the interatomic bonding of the Mg_9Si_5 phase is weakened, resulting in a decrease in material hardness. In particular, the atomic bond of $Mg_{17}Si_{10}Zn$ compound is the weakest, indicating that the doping of the Zn element reduces the strength of the Mg_9Si_5 phase and enhances its toughness. These results are consistent with the mechanical modulus analysis described above. Next, we discuss in detail the effects of different elements doped on Mg_9Si_5 phase from an electronic perspective.

Electronic structure properties

In order to gain a deeper understanding of how doping elements affect the bonding stability and mechanical properties of Mg_9Si_5 phase at the electronic level, we conducted an analysis of the electronic partial density of states (PDOS) of the doping atom and its nearest neighbor atoms. Fig. S1 shows the nearest neighbors of Mg2 atom, which are Si1 and Si2a atoms, and Fig. 2 plots the PDOS of these four types of atoms.

In the energy range from − 6 eV to the Fermi level, a noteworthy orbital hybridization was observed between the *s* and *p* orbitals of the Si1, Si2a, and Mg2 atoms. In particular, the *p* orbitals of the Si1 and Si2a atoms displayed greater contribution in this energy range, as depicted in Fig. 2(a). The *s* orbital electrons of the Si1 and Si2a atoms exhibit high electron occupancy peaks within the energy level range of − 10 eV to − 8 eV, but the Si1-*s* and Si2a-*s* orbitals do not produce significant overlapping peaks. The properties of the pristine Mg_9Si_5 phase are mainly determined by the Si atom, as the Mg atom has a lower peak valence electron orbital. Our findings are consistent with those obtained by V. Singh et al., who reported that the DOS of Mg and Si atoms in the Mg_9Si_5 phase are distributed in a wide energy range, with the Si-3*p* states dominating near the Fermi energy.[4]

Figure 2(b)–(c) demonstrate that the doping of Ca and Sr atoms does not affect the PDOS distribution of Si1, Si2a, and Mg2 atoms around them. This is due to the low peak electron occupancy of these two atoms below the Fermi level, making it difficult for them to form new hybrid states that affect the bonding performance of the Mg_9Si_5 phase. This also explains why the mechanical properties of $Mg_{17}Si_{10}Ca$ and $Mg_{17}Si_{10}Sr$

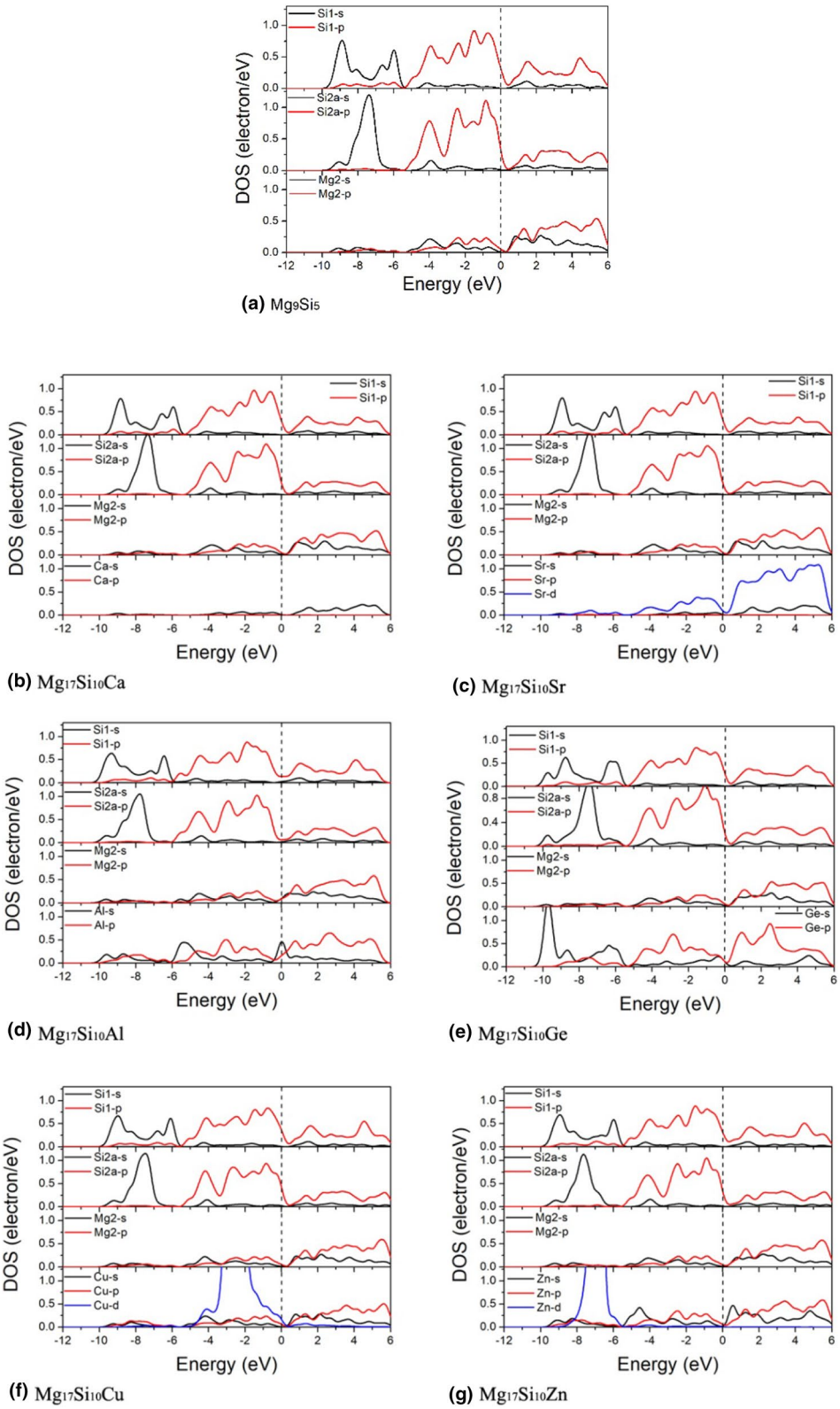

Figure 2. (a) The PDOS of Mg_9Si_5 structure. (b–h) The PDOS of $Mg_{17}Si_{10}X$ structures (X=Ca, Sr, Al, Ge, Cu, Zn).

compounds are as similar as the pristine Mg_9Si_5. As for the $Mg_{17}Si_{10}Cu$ compound, while the Cu-*d* electrons in Fig. 2(f) have a higher peak contribution in the energy range from − 4 eV to the Fermi level, the peaks of Cu–*s* and Cu-*p* electrons always occupy the lower energy range. This suggests that the hybridization of Cu-*d* with Si1-*p* and Si2a-*p* orbitals has some effects on the properties of the pristine phase. Subsequent analysis shows that $Mg_{17}Si_{10}Cu$ compound has lower mechanical properties (B, E, H_v) and better toughness and ductility than the pristine phase because the distribution of electron orbitals of Cu atoms mainly appears below the Fermi level, and the PDOS contribution of Cu atoms is slightly higher than that of Ca and Sr atomic orbitals. In Fig. 2(d), (e), and (g), the addition of doping atoms such as Al, Ge and Zn alters the mechanical properties of the pristine phase, such as lower modulus, lower Vickers hardness and higher Poisson's ratio, when the peak distribution of electron PDOS from the Fermi level to − 10 eV is greater than the contribution of adjacent Mg atoms. This change in performance is attributed to the hybridization of the X-*p* and Si-*p* orbitals, especially the Zn-*d* and Si2a-*s* orbitals, which create high hybridization peaks in the energy level range of − 8 eV to − 6 eV. The properties of $Mg_{17}Si_{10}Zn$ differ significantly from the other five $Mg_{17}Si_{10}X$ compounds and pristine phases due to the significant peak contribution of hybridization below the Fermi level. Consequently, we posit that doping elements have a higher contribution of *s* electron and *p* electrons at the Fermi level, and they can form hybrid peaks with Si-*s* orbitals at low levels. This mechanism is responsible for the toughness and ductility of the Mg_9Si_5 phase on a microscopic level.

In order to further investigate the effect of doping elements on the bonding stability and fracture properties, we analyzed the electron density difference (EDD) of the pristine Mg_9Si_5 phase and $Mg_{17}Si_{10}X$ compounds. Figure 3(a) shows the EDD projection plane of the pristine Mg_9Si_5 phase, and Fig. 3(b) shows the corresponding sections. The EDD shows a significant charge accumulation in the atomic space of the pristine Mg_9Si_5 phase, with Si1–Mg2 and Si2a–Mg2 forming covalent bonds and Mg2–Mg2 forming metallic bonds. Figure 3(c)–(h) show the covalent bonds between Si1 and Si2a atoms and doping atoms in the $Mg_{17}Si_{10}X$ compounds. Quantitative analysis of EDD color shows that the order of Si-X covalent bonds strength is Si–Al > Si–Sr > Si–Ca > Si–Ge > Si–Zn > Si–Cu, while the order of Mg2-X metallic-like bonds are Mg2–Ca > Mg2–Sr > Mg2–Ge > Mg2–Zn > Mg2–Cu > Mg2–Al. However, some Mg2-X bonding types exhibit significant changes, with Mg2–Ca and Mg2–Sr bonds changing from metal bonds to ionic bonds, causing charge to be lost around Mg2 atoms and transferring to doped Ca or Sr atoms. These new bonds will influence the mechanical properties together with the Si-X covalent bonds. Moreover, the strength of Mg2–Mg2 bond of pristine Mg_9Si_5 is stronger than that of the Mg2–Ge, Mg2-Zn and Mg2–Cu bonds in $Mg_{17}Si_{10}X$ compounds, leading these compounds have lower Young's modulus and Vickers hardness. Despite having the greatest strength of Si-X covalent bonds, but the weak and split Mg2–Al bonds lead to the ability to cause resistance in each direction of the compound is different, so its shear model, Young's model and Vickers hardness are not high. As the PDOS analysis showed, the properties of the Mg_9Si_5 phase are mainly determined by the Si and Mg2 atoms. Therefore, the covalent bond between Si–X and Si–Mg is the main factor determining the mechanical properties of the $Mg_{17}Si_{10}X$ compounds, while the Mg2-X bond is a secondary factor.

It is evident that the EDD provides an estimate of the difference between charge gain and loss in a material's sheet. To further investigate the amount of charge transfer within the material's inner space, we can utilize the Bader charge analysis. Table SIV displays the average Bader charges of dopant X atoms and their nearest neighbors in pristine Mg_9Si_5 and $Mg_{17}Si_{10}X$ compounds. For Mg_9Si_5 phase, Mg atoms lose approximately 3.4*e* charge, while Si1 and Si2 atoms gain approximately 2.0*e* and 3.0*e* charge, respectively. In the $Mg_{17}Si_{10}Ca$ and $Mg_{17}Si_{10}Sr$ compounds, the amount of charge lost by the Mg atoms is quite similar to that lost in the pristine phase, leading to Si atoms gaining charge from the dopant atom. Consequently, the Ca and Sr atoms lose 1.264*e* and 1.193*e*, respectively. When the Mg atoms in the $Mg_{17}Si_{10}X$ compound lose the same amount of charge as the pristine phase, but with Si atoms gaining less charge, the excess charge can only be transferred from the doped element to the surrounding area. Therefore, Ge and Cu atoms in the $Mg_{17}Si_{10}Ge$ and $Mg_{17}Si_{10}Cu$ compounds capture 0.074*e* and 0.452*e* charges, respectively. However, a unique result occurs in the $Mg_{17}Si_{10}Al$ and $Mg_{17}Si_{10}Zn$ compounds, where Mg atoms lose nearly the same amount of charge as the pristine phase, but the Si atoms gain significantly less charge, especially in the case of Zn-doped. Al and Zn atoms donate 0.862*e* and 0.138*e* charges, respectively, to the surrounding atoms as electron donors. The data reveal that the charge given by Mg atoms in the two doped compounds is unevenly distributed to Al or Zn atom. This discrepancy may arise because the statistical mean cannot accurately reflect the charge transfer in the local environment around the doping elements. Consequently, Mg around the Al or Zn atoms obtains much higher charges (3.431*e* and 3.446*e*) than the average. However, the Mg atom far away from the doping atom mainly acquires charge from the surrounding Si atom, and its required charge is lower than the mean 2.0*e* and 3.0*e* given by Si. Overall, the electron orbital of Si atom is the most important parameter affecting the properties of the $Mg_{17}Si_{10}X$ compounds. Additionally, the material's strength-ductility can be fine-tuned by changing the charge transfer around the dopant atom.

Conclusion

The study investigates the pristine β'-Mg_9Si_5 and role of various doping elements such as Ca, Sr, Al, Ge, Cu, and Zn through first-principles density-functional calculations. The effects of different doping elements and sits are examined by constructing and comparing 12 crystal models. Formation enthalpy and cohesive energy calculations reveal that Mg2 site is the most

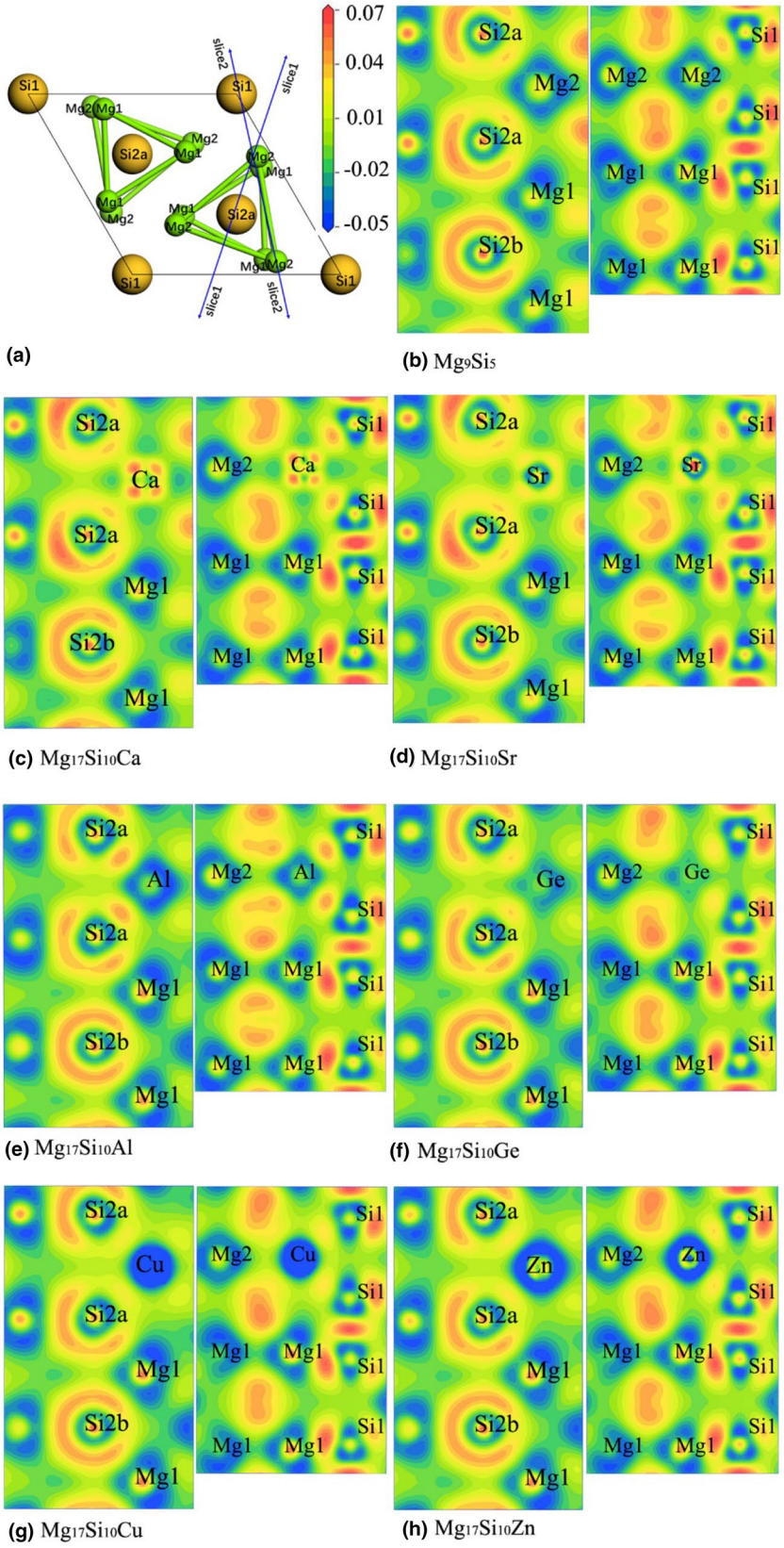

Figure 3. The electron density difference (EDD) Mg_9Si_5 and $Mg_{17}Si_{10}X$ structures (X=Ca, Sr, Al, Ge, Cu, Zn). (a) Schematic diagram of slices in the crystal cell of Mg_9Si_5. (b) Two EDD slices of Mg_9Si_5. (c–h) The EDD slices of $Mg_{17}Si_{10}X$ structures (X=Ca, Sr, Al, Ge, Cu, Zn).

stable configuration. The formation enthalpies for $Mg_{17}Si_{10}X$ compounds are found to vary, with $Mg_{17}Si_{10}Ge$ exhibiting the highest degree of enlargement followed by $Mg_{17}Si_{10}Al$, $Mg_{17}Si_{10}Cu$, $Mg_{17}Si_{10}Sr$, and $Mg_{17}Si_{10}Zn$.

The study also investigates the elastic and mechanical properties of the pristine Mg_9Si_5 phase and the doped $Mg_{17}Si_{10}X$ compounds.

It is observed that the doping of Ge, Cu and Zn elements can slightly increase the brittleness of the pristine Mg_9Si_5 phase. On the other hand, the doping of Ca and Sr elements can improve the ductility of Mg_9Si_5 phase while losing less strength. The Vickers hardness of Mg_9Si_5 phase decreases due to doping, particularly for $Mg_{17}Si_{10}Al$ and $Mg_{17}Si_{10}Zn$ compounds. Among all the compounds, $Mg_{17}Si_{10}Zn$ exhibits the strongest resistance to crack initiation.

The study investigates the impact of doping atoms through an analysis of their Bader charge and PDOS. The PDOS curves reveal that the doping element contributes a significant amount of X-*s* and X-*p* electrons at the Fermi level, leading to the formation of a hybrid peak with the Si-*s* orbital at the lower energy level. The properties of Mg_9Si_5 and the $Mg_{17}Si_{10}X$ compounds are primarily determined by the electron orbits of Si atoms. The strength of the Si-X covalent bond follows the order Si–Al > Si–Sr > Si–Ca > Si–Ge > Si–Zn > Si–Cu. The covalent bond between Si-X and Si–Mg is the primary factor that influences the mechanical properties of $Mg_{17}Si_{10}X$ compounds, while the Mg2-X bond plays a secondary role.

Acknowledgments

The authors gratefully acknowledge the financial support of this study from the Fundamental Research Funds for the Central Universities (FRF-GF-20-25B). This work is also thankful for the Research Program of Beijing Municipal Education Commission (Nos. KM201910037001, KM201910037186).

Funding

Fundamental Research Funds for the Central Universities, FRF-GF-20-25B, Chuan-Hui Zhang, Beijing Municipal Education Commission, KM201910037001, Lianhong Ding, KM201910037186, Lianhong Ding

Data availability

The datasets generated during and/or analyzed during the current study are available from the corresponding author on reasonable request.

Declarations

Conflict of interest

The authors have no conflicts of interest.

Supplementary Information

The online version contains supplementary material available at https://doi.org/10.1557/s43579-023-00427-1.

References

1. G.L. Mao, S.G. Liu, W.L. Gao, J. Wang, D.Y. Liu, Effect of Zn or Zn + Cu addition on the precipitation in Al-Mg-Si alloys: a Review. Trans. Indian Inst. Met. **74**, 2925 (2021)
2. R. Vissers, M.A. Van Huis, J. Jansen, H.W. Zandbergen, C.D. Marioara, S.J. Andersen, The crystal structure of the β′ phase in Al–Mg–Si alloys. Acta Mater. **55**, 3815 (2007)
3. S. Ji, M. Imai, H. Zhu, S. Yamanaka, Structural characterization of magnesium-based compounds Mg_9Si_5 and Mg_4Si_3Al (Superconductor) synthesized under high pressure and high temperature conditions. Inorg. Chem. **52**, 3953 (2013)
4. V. Singh, J.J. Pulikkotil, S. Auluck, Mg_9Si_5: a potential non-toxic thermoelectric material for mid-temperature applications. RSC Adv. **6**, 62445 (2016)
5. Y. Zheng, L.P. Bian, H.L. Ji, X.W. Liu, F. Tian, Influence of Ca and Mn on microstructure, mechanical properties, and electrical conductivity of As-Cast and heat-treated Al–Mg–Si Alloys. Rare Metal Mater. Engin. **51**, 4010 (2022)
6. G.X. Lu, H.J. Chen, S.K. Guan, Effect of Sr on forming properties of Al-Mg-Si based alloy sheets. Trans. Nonferrous Met. Soc. China **16**, s1489 (2006)
7. M. Liu, J. Banhart, Effect of Cu and Ge on solute clustering in Al–Mg–Si alloys. Mater. Sci. Engin. A **658**, 238 (2016)
8. R. Bjørge, S.J. Andersen, C.D. Marioara, J. Etheridge, R. Holmestad, Scanning transmission electron microscopy investigation of an Al–Mg–Si–Ge–Cu alloy. Philos. Mag. **92**, 3983 (2012)
9. F. Glöckel, P.J. Uggowitzer, P. Felfer, S. Pogatscher, H.W. Höppel, Influence of Zn and Sn on the precipitation behavior of new Al–Mg–Si Alloys. Materials **12**, 2547 (2019)
10. M.J. Yang, A. Orekhov, Z.Y. Hu, M. Feng, S.B. Jin, G. Sha, K. Li, V. Samaee, M. Song, Y. Du, G. Van Tendeloo, D. Schryvers, Shearing and rotation of β″ and β′ precipitates in an Al–Mg–Si alloy under tensile deformation: In-situ and ex-situ studies. Acta Mater. **220**, 117310 (2021)
11. M. Tamizifar, and G. W. Lorimer. Proc. 3rd Int. Conf. on Aluminium Alloys: Their Physical and Mechanical Properties, ed. L. Arnberg, O. Lohne, E. Nes and N. Ryum, 220 (1992)
12. C. Ravi, C. Wolverton, First-principles study of crystal structure and stability of Al–Mg–Si–(Cu) precipitates. Acta. Mater. **52**, 4213 (2004)
13. D. Zhao, L. Zhou, Y. Kong, A.J. Wang, J. Wang, Y.B. Peng, D. Yong, Y.F. Ouyang, W.Q. Zhang, Structure and thermodynamics of the key precipitated phases in the Al–Mg–Si alloys from first-principles calculations. J. Mater. Sci. **46**, 7839 (2011)
14. H. Zhang, Y. Wang, S.L. Shang, C. Ravi, C. Wolverton, L.Q. Chen, Z.K. Liu, Solvus boundaries of (meta) stable phases in the Al–Mg–Si system: first-principles phonon calculations and thermodynamic modeling. Calphad **34**, 20 (2010)
15. T. Saito, E.A. Mørtsell, S. Wenner, C.D. Marioara, S.J. Andersen, J. Friis, Matsuda, K.R. Holmestad, Atomic structures of precipitates in Al–Mg–Si alloys with small additions of other elements. Adv. Eng. Mater. **20**, 1800125 (2018)
16. M.D. Segall, P.J.D. Lindan, M.J. Probert, C.J. Pickard, P.J. Hasnip, S.J. Clark, M.C. Payne, First-principles simulation: ideas, illustrations and the CASTEP code. J. Phys. Condens. Matter. **14**, 2717 (2002)
17. J.P. Perdew, Y. Wang, Accurate and simple analytic representation of the electrongas correlation energy. Phys. Rev. B. **45**, 13244 (1992)
18. H.J. Monkhorst, J.D. Pack, Special points for Brillouin-zone integrations. Phys. Rev. B. **16**, 1748 (1976)
19. T.H. Fischer, J. Almlof, General methods for geometry and wave function optimization. J. Phys. Chem. **96**, 9768 (1992)
20. G. Henkelman, A. Arnaldsson, H. Jónsson, A fast and robust algorithm for Bader decomposition of charge density. Comput. Mater. Sci. **36**, 354 (2006)

21. M.A. Van Huis, J.H. Chen, H.W. Zandbergen, M.H.F. Sluiter, Phase stability and structural relations of nanometer-sized, matrix-embedded precipitate phases in Al-Mg-Si alloys in the late stages of evolution. Acta. Mater. **54**, 2945 (2006)
22. D.G. Clerc, H.M. Ledbetter, Mechanical hardness: a semiempirical theory based on screened electrostatics and elastic shear. J. Phys. chem. Solids. **59**, 1071 (1998)
23. B. Zhang, L. Wu, B. Wan, J. Zhang, Z. Li, H. Gou, Structural evolution, mechanical properties, and electronic structure of Al–Mg–Si compounds from first principles. J. Mater. Sci. **50**, 6498 (2015)
24. B.K. Li, J.K. Wang, C.H. Zhang, First-principles study on the effects of V, Nb, Cd, Ag, Ge and Sb doped in Al2CuMg phase of Al–Zn–Mg-Cu alloy. Mod. Phys. Lett. B. **35**, 2150478 (2021)
25. S.F. Pugh, Relations between the elastic moduli and the plastic properties of polycrystalline pure metals. Philos. Mag. Ser. **45**, 823 (1954)
26. Y.J. Tian, B. Xu, Z.S. Zhao, Microscopic theory of hardness and design of novel superhard crystals. Int. J. Refract. Metals. Hard. Mater. **33**, 93 (2012)
27. Y. Liu, W.C. Hua, D.J. Li, K. Li, H.L. Jin, Y.X. Xu, C.S. Xu, X.Q. Zeng, Mechanical, electronic and thermodynamic properties of C14 type AMg_2 (A=Ca, Sr, Ba) compounds from first principles calculations. Comput. Mater. Sci. **97**, 75 (2015)
28. O.L. Anderson, Determination and some uses of isotropic elastic constants of polycrystalline aggregates using single-crystal data. Phys. Acoustics. **3**, 43 (1965)
29. B. Chen, B.K. Li, J.K. Wang, C.H. Zhang, DFT investigation on the rare earth effects of Mg_8Si_3RE (RE=Sc, La, Ce, Yb) compounds. Solid. State. Commun. **330**, 114269 (2021)
30. N.A. Gaida, K. Niwa, T. Sasak, M. Hasegawa, Phase relations and thermoelasticity of magnesium silicide at high pressure and temperature. J. Chem. Phys. **154**, 144701 (2021)

Publisher's Note Springer Nature remains neutral with regard to jurisdictional claims in published maps and institutional affiliations.

Springer Nature or its licensor (e.g. a society or other partner) holds exclusive rights to this article under a publishing agreement with the author(s) or other rightsholder(s); author self-archiving of the accepted manuscript version of this article is solely governed by the terms of such publishing agreement and applicable law.